




Original Article

Residual strain investigation of a polycrystalline quartzite rock sample using time-of-flight neutron diffraction

Altangerel Badmaarag<sup>1,2</sup> \* , Deleg Sangaa<sup>1</sup> , Vadim V. Sikolenko<sup>2,3</sup> , Lkhamsuren Enkhtur<sup>4</sup> 

<sup>1</sup>Department of Physics, Institute of Physics and Technology, Mongolian Academy of Sciences, Ulaanbaatar 210651, Mongolia

<sup>2</sup>Department of Neutron Investigations of Condensed Matter, Frank Laboratory of Neutron Physics, Joint Institute for Nuclear Research, Dubna 141980, Russia

<sup>3</sup>Division Technical Petrophysics, Institute of Applied Geosciences, Karlsruhe Institute of Technology, Karlsruhe 76131, Germany

<sup>4</sup>Department of Physics, School of Art and Sciences, National University of Mongolia, Ulaanbaatar 14200, Mongolia

\*Corresponding author: [badmaarag0815@gmail.com](mailto:badmaarag0815@gmail.com), ORCID: [0009-0001-8439-8292](https://orcid.org/0009-0001-8439-8292)

ARTICLE INFO

Article history:

Received 27 December, 2022

Revised 21 March, 2023

Accepted 09 July, 2023

ABSTRACT

In this work, we studied the residual micro lattice strain of an onyx sample, which is a micro- to the cryptocrystalline variety of the mineral quartz  $\text{SiO}_2$ . That the investigation has been carried out using in-situ stress experiments with the time-of-flight neutron diffraction method. The aim of the study is to investigate residual lattice strains and pressure directions in the sample using time-of-flight neutron diffraction, which is a powerful tool for the study of the residual strain behavior in bulk materials, like geological rock samples containing large grains. The residual strain was detected in different sample directions turning the sample in steps of  $30^\circ$  by  $180^\circ$  around the cylindrical z-axis. These experiments have been performed at the time-of-flight neutron strain diffractometer EPSILON, situated on the pulsed neutron source IBR-2M of the Joint Institute for Nuclear Research in Dubna, Russia. The results of this study will provide insights into the compressional and tensional residual strain of the crystallographic lattice planes, and will have implications for our understanding of the tectonic history of this region. These different strains are arranged in the sample by a sinusoidal distribution in radial directions.

**Keywords:** Time-of-flight (TOF) method, residual strain, Reitveld refinement, earthquakes

INTRODUCTION

Diffraction techniques are widely used in the study of the mechanical properties of crystal structures of materials, rocks, and minerals. Quartz constitutes a large volume of the earth's upper crust, which is about 59-60 percent. Therefore, studies of quartz and quartz-containing rocks are important for explaining some of the effects of seismicity (Genyao et al., 2013). The distribution of earthquake impacts depends on the tectonic stress field of the earth and on the crystal and the mechanical properties of the rocks and rock layers (Cunningham,

2017; Genyao et al., 2013).

Due to the effects of stress, the crystalline structure of the substance is somewhat deformed resulting in residual strain within the crystal lattice even after the stress is released due to earthquakes or reduced due to changes in tectonic stress (Frischbutter et al., 2000). Because the distribution of mechanical and crystalline structural changes in the earth's crust is related to the distribution of terrestrial tectonic stress, the study of the physical properties of the crystalline phase in terms of

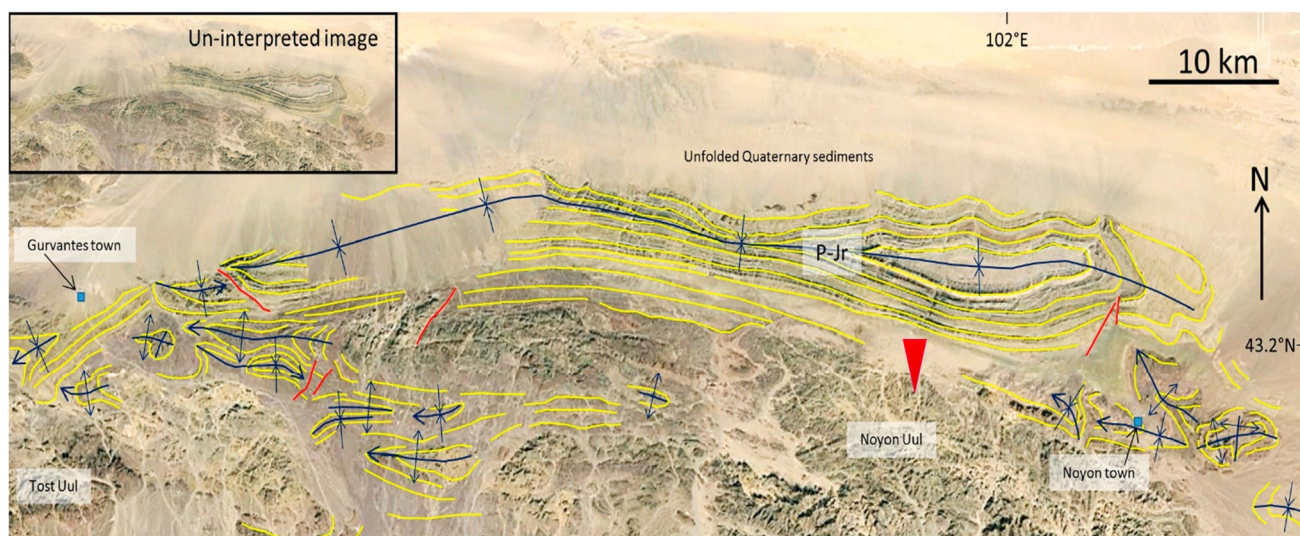
© The Author(s). 2022 **Open access** This article is distributed under the terms of the Creative Commons Attribution 4.0 International License (<https://creativecommons.org/licenses/by/4.0/>), which permits unrestricted use, distribution, and reproduction in any medium, provided you give appropriate credit to the original author(s) and source, provide a link to the Creative Commons license, and indicate if changes were made.

pressure, temperature, or thermodynamic conditions is of great importance (Schäfer, 2002; Friedman, 1972). The results presented in our paper were performed on the EPSILON neutron diffractometer instrument at the IBR-2 reactor, Joint Institute for Nuclear Research, Dubna, Russia (Taran et al., 2014; Scheffzük et al., 2016). The ONYX rock sample is a trigonal crystal system low-temperature alpha-quartz.

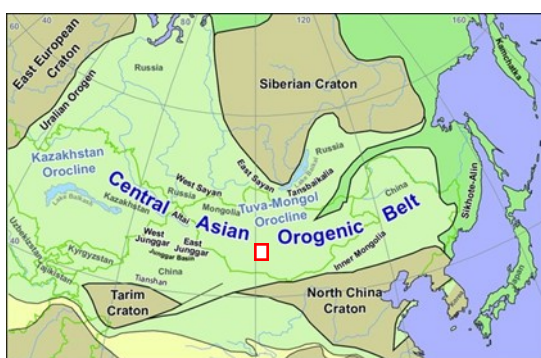
In this study, we investigate an onyx sample (a micro- to a cryptocrystalline variety of the mineral quartz) collected from the south Mongolian mountain region in order to understand the residual micro lattice strain of rock sample and use in-situ stress experiments with the time-of-flight (TOF) neutron diffraction method.

## GEOLOGICAL SETTINGS AND SAMPLE DESCRIPTION

CAOB is a complex tectonic unit that originated in the Phanerozoic and became its final structure through the closure of the Permian-Triassic Solonker suture in northernmost China and the Jurassic Mongol-Okhotsk suture in northeast Mongolia and eastern Siberia (Cunningham, 2017). In southern Mongolia these tectonic events were followed by the crustal extension of a widespread Cretaceous Basin. Therefore, Cretaceous to late Cenozoic elastic sedimentary deposits overlie older, deformed Permian-Jurassic sedimentary rocks associated with the Permian-Triassic-Solonker and Jurassic-Mongol-Okhotsk collision lines (Cunningham, 2017), (Fig. 1a).



a)



b)



c)

**Fig. 1.** a). Tectonic structure of the Permo-Jurassic sedimentary layers in Noyon mountain region. This folded Permian-Jurassic rock layers (bedding traces-yellow lines) are unconformable overlapped by Cretaceous-Quaternary clastic sediments. Major fold hinges (dark blue lines) in Permian-Jurassic (P- J) rocks, red lines are faults. Sample location-red arrow (Cunningham, 2017). b) Location of Noyon mountain in Umnugobi province (Windley and Xiao, 2018). c) Drilled cylindrical onyx sample (60 mm in length, 30 mm diameter) from the Noyon mountain (43°8'54"N, 102°7'38"E).

From Miocene to recent times transpressional left lateral movement associated with the reactivation of the old fracture systems of the CAOB prevails (Cunningham, 2017; Schlupp and Cisternas, 2007). This still continuing tension in the whole Gobi-Altai region is attributed to the ongoing colliding of India with South Asia in the northeast (Cunningham, 2017). The E- to SE- motion of central and eastern Mongolia is actually accommodated by left-lateral slip on the E-W trending Tunka, Bolnay and Gobi-Altai faults ( $2 \pm 1.2$  mm/yr,  $2.6 \pm 1.0$  mm/yr, and  $1.2$  mm/yr, respectively) (Calais et al., 2003). Tectonic stress is currently discharged along those and other Quaternary northwest-trending thrust faults and east-west sinistral strike-faults, which initiated a series of strong earthquakes with magnitude  $M_w > 8$  across the region in the recent past (Tsetserleg earthquake (1905 Jul. 9), Bolnay earthquake (1905 Jul. 23) and Gobi-Altai earthquake (1957 Dec. 4)) (Schlupp and Cisternas, 2007). The studied a micro- to a cryptocrystalline variety of the mineral quartz onyx sample derives from Noyon Mountain in the Umnugobi province, which is a part of the Central Asian Orogenic Belt (CAOB) (Fig. 1b), (Cunningham, 2017; Windley and Xiao, 2018), and shows

traces of fracture strain (Fig. 1c) resulting from recent tectonic activity in the Noyon mountain region. The effects of these tectonic processes are contained in the form of the residual strain and can be detected using neutron diffraction measurements.

## METHODS

The measurements of the sample were performed at the neutron diffractometer EPSILON. The application of neutron diffraction methods allows strain detection in the crystallographic lattice spacing. Furthermore, the method allows detecting the strain for each mineralogical phase in the samples. Diffraction is based on Bragg's law (Eq. 1)

$$2d_{hkl} \sin\theta = n\lambda \quad (1)$$

with  $d_{hkl}$  -lattice spacing (m),  $\theta$  -Bragg angle ( $^\circ$ ),  $\lambda$  -wavelength (m), diffraction order  $n \in \mathbb{N} \setminus \{0\}$ .

The pulsed neutron source with the TOF method allows the investigation of the lattice distance (Eq. 2) by

$$d_{hkl} = \frac{h}{2m_n L \sin\theta} \cdot t \quad (2)$$

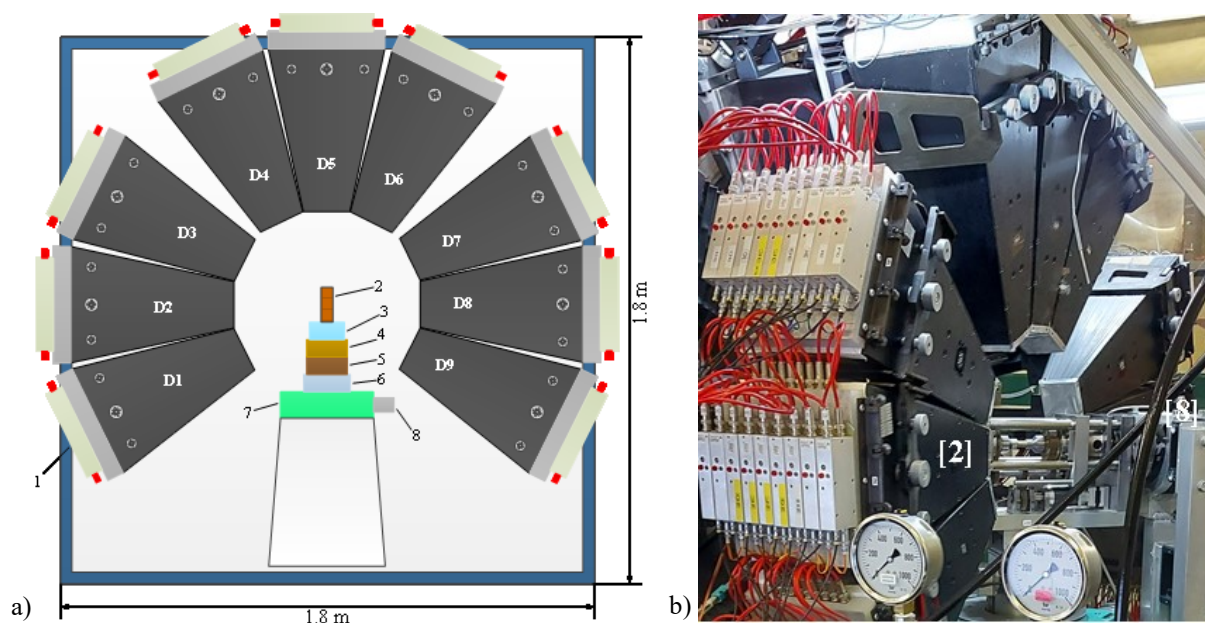


**Fig. 2.** a) Scheme of Epsilon diffractometer: 1 -block detectors (D1-D9), 2 -sample, 3-8 -goniometer, b) The neutron TOF strain/stress diffractometer at the pulsed source IBR-2M, equipped with 9 block detectors at a scattering angle of  $2\theta=90^\circ$  around the incident neutron beam.

with  $h$  -Planck's constant,  $m_n$  -mass of the neutron (kg),  $L$  -total flight path (m),  $t$  -TOF(s). The lattice strain can be determined using the equation Eq. 3:

$$\langle \varepsilon_{hkl} \rangle = \frac{\langle d_{hkl} \rangle - d_{hkl}^0}{d_{hkl}^0} \quad (3)$$

With  $\langle \varepsilon_{hkl} \rangle$  -strain in sample direction  $[hkl]$  (dimensionless),  $\langle d_{hkl} \rangle$  -lattice spacing in a sample direction  $[hkl]$  (m),  $d_{hkl}^0$  -lattice spacing of the strain-free state (m). The neutron TOF strain diffractometer Epsilon is designed for the investigation of residual and applied intra-crystalline strain bulk samples. The neutron source IBR-2M is pulsed with a frequency of 5 Hz. Based on the long neutron flight path of about 107 m, a high resolution is achieved, which allows the investigation of multiphase materials and the investigation of phases with lower crystal symmetry.

Because of the large wavelength-range ( $\lambda=7.8$  Å)  $d$  -spacings up to  $d=5.3$  Å can be investigated. The diffractometer is equipped with a uniaxial pressure device, allowing load states up to 100 kN, i.e.  $\approx 140$  MPa using a sample diameter of 30 mm and 60 mm length (Scheffzük et al., 2012). (Fig. 2).

The strain investigation using neutron diffraction at the EPSILON strain diffractometer enables:

1. The determination of lattice planes in the range up to 5.3Å spacing
2. The detection of first and second order strain, i. e. The detection of macro and micro strain, which is contained in the Bragg peak position and in the peak shape parameter Full Width at Half Maximum (FWHM),
3. The determination of residual strain without external load,
4. The determination of applied load with a uniaxial maximal load up to 100 kN ( $\sim 150$  MPa for cylindrical samples with 30 mm in diameter),
5. The investigation of thermal residual strain,
6. Using the method of strain scanning by selecting gauge volumes ( $\text{cm}^3$ ) differently located in the sample, the spatial distribution of the strain in the sample can be resolved.

## EXPERIMENTAL SETUP AND RESULTS

The block detectors {2} and {8} at the strain diffractometer EPSILON are in opposite positions, allowing the measurement of two perpendicular directions characterized by the scattering vectors  $Q_2$  and  $Q_8$  (Fig. 3).

The resulting TOF neutron diffraction pattern demonstrates the range of lattice spacing on a quartz sample. The diffraction pattern plotted relating its lattice spacing only from 0.5 to 3.5 Å. Some Bragg reflections of the trigonal quartz are indexed. The neutron cross-sectional area is adjusted to a dimension of 50 mm x 15 mm by a special diaphragm and the residual deformation is determined using the measurement value of the {2} and {8} block detectors on the EPSILON diffractometer's schematic (Scheffzük et al., 2016). The spectrum of the TOF neutron diffraction is refined by detailed crystal structure parameters, calculated by the Rietveld method of polycrystalline crystalline structure and strain (Rietveld, 1967). Fig. 4 shows the neutron TOF diffraction pattern of rock sample ONYX refined by the Rietveld refinement and profile analysis method. The homogenous strain is characterized by the elastic properties of the monocrystalline and Young's module  $E$ , which is characterized by the transformation of the neutron diffraction of the change peak shapes, the extension, and the maximum peak of the position displacement (Scheffzuek et al., 2014).

Results of neutron diffraction profile and Rietveld analysis and residual strain in each of

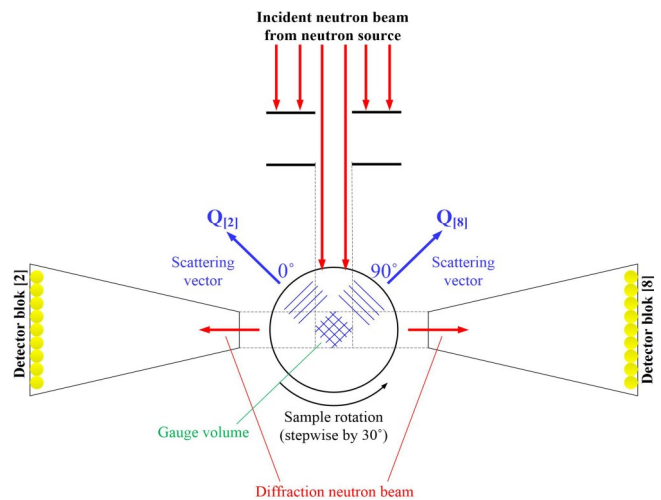
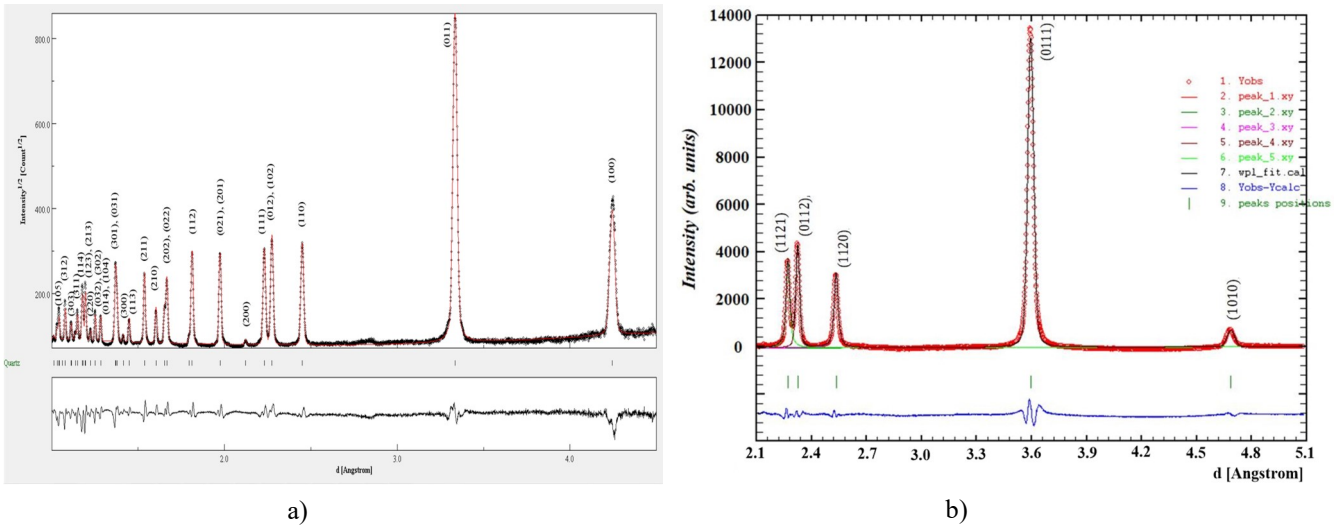
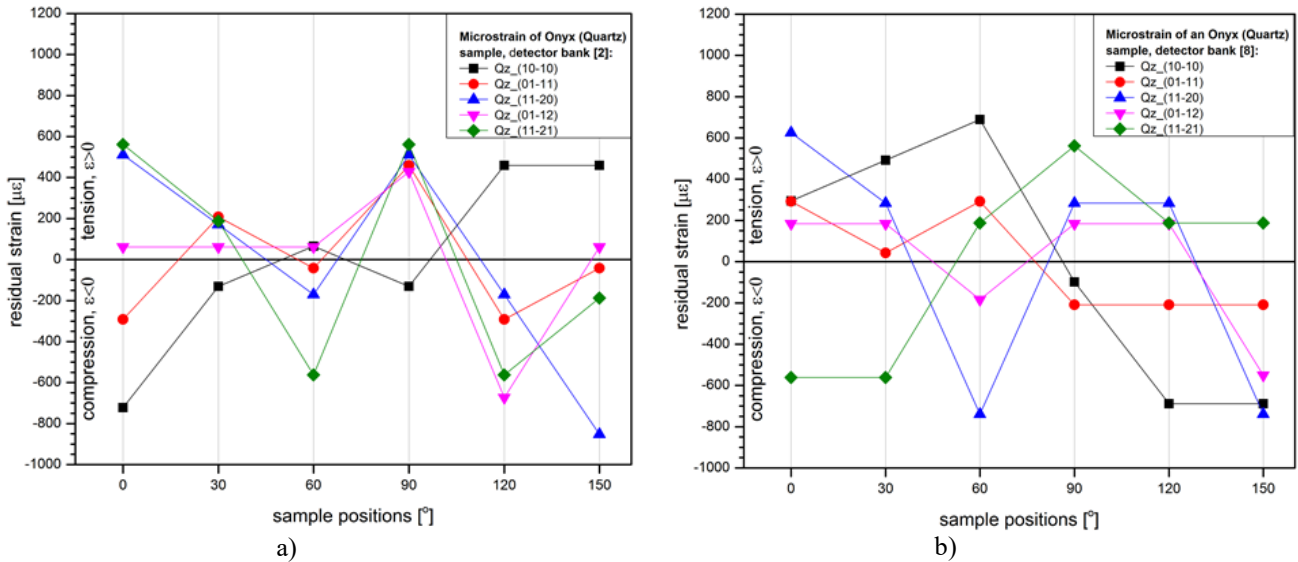


Fig. 3. Measurement schematic of EPSILON diffractometer



**Fig. 4.** The Rietveld refinement (a) and peak profile analysis (Wenk et al., 2010) (b) of the TOF neutron diffraction from the ONYX sample.



**Fig. 5.** Residual strain in crystalline structures depending on the pressure and other factors of ONYX is estimated for five different crystalline planes. a) Residual strain in axial direction, b) residual strain in radial direction

the measurement locations are shown in Figs. 4 and 5. The neutron TOF diffraction pattern demonstrates the range of lattice spacing on a quartzite rock sample (Fig. 4a). The diffraction pattern plotted relating its lattice spacing only from 2.1 to 4.5 Å (Fig. 4b). The high-intensity Bragg peaks of trigonal quartz are indexed (Fig. 4).

The strain values of the Bragg reflections (10 $\bar{1}$ 0), (01 $\bar{1}$ 1), (11 $\bar{2}$ 0), (01 $\bar{1}$ 2), (11 $\bar{2}$ 1) are given in Fig. 5.

They indicate that the correction of the crystallization in the measurement sites has

occurred. The crystal lattice space (geologic sample) change is the distance between the planes that affects the effects of an earthquake or some pressure.

The residual strain scans show that the strain is inhomogeneous and it has the highest distribution along y axis. Besides, crystal planes (10 $\bar{1}$ 0), (11 $\bar{2}$ 0) in the axial direction have maximum values from -721.98 $\mu\epsilon$  to 459.44 $\mu\epsilon$  (compression to tension) and from 511.51 $\mu\epsilon$  to -852.52 $\mu\epsilon$  (tension to compression), respectively.

But negative to positive strains (compression - tension) were detected for crystal planes  $(10\bar{1}0)$ ,  $(01\bar{1}1)$ ,  $(11\bar{2}0)$ ,  $(01\bar{1}2)$  perpendicular to  $y$ -axis, and positive to negative strains were detected (tension-compression) for crystal plane  $(11\bar{2}1)$  (Fig. 5).

The calculated Young's module of the Bragg reflections are different for each plane while having the identical lattice spacing, and these are contrasted with the trigonal quartzite's theoretical values. Table 1 displays the Young's modules  $E$  as obtained by linear regressions (Scheffzuek et al., 2014).

**Table 1.** The obtained Young's modules of the lattice planes  $(10\bar{1}0)$ ,  $(01\bar{1}1)$ ,  $(11\bar{2}0)$ , and  $(11\bar{2}1)$ .

Lattice plane	Young's module $E$	
	Determined [GPa]	Theoretical [GPa]
$(10\bar{1}0)$	$59.9 \pm 2.5$	76.4
$(01\bar{1}1)$	$66.2 \pm 3.0$	83.4
$(11\bar{2}0)$	$72.7 \pm 6.1$	78.2
$(01\bar{1}2)$	$60.1 \pm 4.7$	93.2
$(11\bar{2}1)$	$65.7 \pm 3.8$	89.0
	$\bar{E} = 64.92 \pm 4.02$	$\bar{E} = 84.04 \pm 2.4$

## DISCUSSION AND CONCLUSION

The strain investigation of bulk material samples with coarse grains and phases of lower crystal symmetry requires a diffraction method with a high penetration depth and high spectral resolution. The TOF neutron diffraction fulfills these requirements and thus is suitable.

- The strain was determined using in-situ strain experiments on an ONYX rock sample. For a given direction of the sample compression, lattice strain values were measured for the crystallographic  $(10\bar{1}0)$ ,  $(01\bar{1}1)$ ,  $(11\bar{2}0)$ ,  $(01\bar{1}2)$ , directions and Young's module of the listed Bragg reflections show lower values than theoretically determined for the sample. It varies depending on the admixture and

chemical composition of the accompanying elements, such as those causing the color of the sample.

- A tensional residual strain from  $\mu\epsilon_{axial} = 61.19$  to  $561.9$ ,  $\mu\epsilon_{lateral} = 41.73$  to  $689.05$ , and a compressional residual strain from  $\mu\epsilon_{axial} = -41.75$  to  $-852.52$ ,  $\mu\epsilon_{lateral} = -98.43$  to  $-738.68$  has been detected.
- The direction of maximum compression residual strain in the sample is along the  $[y]$ -axis, and maximum tension residual strain is along the  $[x]$ -axis. This indicates that the direction of the seismic force is along  $[y]$ -axis (directed to north and northwest).

## ACKNOWLEDGEMENTS

We acknowledge also the Institute of Physics and Technology of the Mongolian Academy of Sciences, Frank Laboratory of Neutron Physics at the Joint Institute for Nuclear Research in Dubna, Russia and Karlsruhe Institute of Technology, Karlsruhe, Germany.

## REFERENCES

- Calais, E., Vergnolle, M., San'kov, V., Lukhnev, A., Miroshnitchenko, A., Amarjargal, S., De'verche're J. 2003. GPS measurements of crustal deformation in the Baikal-Mongolia area (1994-2002): Implications for current kinematics of Asia. *Journal of Geophysical Research: Solid Earth*, v. 108(B10), 2501, p. 14.1-14.13. <https://doi.org/10.1029/2002JB002373>
- Cunningham, D. 2017. Folded Basinal Compartments of the Southern Mongolian Borderland: A Structural Archive of the Final Consolidation of the Central Asian Orogenic Belt. *Geosciences*, v. 7(1), p. 2-24. <https://doi.org/10.3390/geosciences7010002>
- Friedman, M. 1972. Residual elastic strain in rocks. *Tectonophysics*, v. 15(4), p. 297-330. [https://doi.org/10.1016/0040-1951\(72\)90093-5](https://doi.org/10.1016/0040-1951(72)90093-5)
- Frischbutter, A., Neov, D., Scheffzük, Ch., Vrána, M., Walther, K. 2000. Lattice strain measurements on sandstones under load using neutron diffraction. *Journal of Structural Geology*, v. 22(11-12), p. 1587-1600. [https://doi.org/10.1016/S0191-8141\(00\)00110-3](https://doi.org/10.1016/S0191-8141(00)00110-3)

- Genyao, W., Yuan, W., Min, L. 2013. Palinspastic reconstruction and geological evolution of Jurassic basins in Mongolia and neighboring China. *Journal of Palaeogeography*, v. 2(3), p. 306-317.
- Rietveld, H.M. 1967. Line profiles of neutron powder-diffraction peaks for structure refinement. *Acta Crystallographica*, v. 22(1), p. 151-152.  
<https://doi.org/10.1107/S0365110X67000234>
- SchäFer, W. 2002. Neutron diffraction applied to geological texture and stress analysis. *European Journal of Mineralogy*, v. 14(2), p. 263-289.  
<https://doi.org/10.1127/0935-1221/2002/0014-0263>
- Scheffzuek, Ch., Hempel, H., Frischbutter, A., Walter, K., Schilling, F.R. 2012. A device for sample rotation under external load for the simultaneous measurement of strain and orientation dependent material properties by means of TOF neutron diffraction. *Journal of Physics Conference Series*, v. 340(1), 012038, p. 1-6.  
<https://doi.org/10.1088/1742-6596/340/1/012038>
- Scheffzuek, Ch., Ullemeyer, K., Vasin, R., Naumann, R., Schilling, F.R. 2014. Strain and Texture Investigations by Means of Neutron Time-of-Flight Diffraction: Application to Polyphase Gneisses. *Material Science Forum*, v. 777, p. 136-141.  
<https://doi.org/10.4028/www.scientific.net/MSF.777.136>
- Scheffzük, Ch., Müller, B., Breuer, S., Badmaarag, A., Schilling, F.R. 2016. Applied strain investigation on sandstone samples using neutron time-of-flight diffraction at the strain diffractometer EPSILON, IBR-2M Dubna. *Mongolian Journal of Physics*, v. 2, p. 433-441.
- Schlupp, A., Cisternas, A. 2007. Source history of the 1905 great Mongolian earthquakes (Tsetserleg, Bolnay). *Geophysical Journal International*, v. 169(3), p. 1115-1131.  
<https://doi.org/10.1111/j.1365-246X.2007.03323.x>
- Taran, Y.V., Balagurov, A.M., Sabirov, B., Davydov, V., Venter, A. 2014. Neutron Diffraction Investigation of Residual Stresses Induced in Niobium-Steel Bilayer Pipe Manufactured by Explosive Welding. *Materials Science Forum*, v. 768-769, p. 697-704.  
<https://doi.org/10.4028/www.scientific.net/MSF.768-769.697>
- Wenk, H.-R., Lutterotti, L., Vogel, S.C. 2010. Rietveld texture analysis from TOF neutron diffraction data. *Powder Diffraction* 25 (3), p. 283-296.  
<https://doi.org/10.1154/1.3479004>
- Windley, B., Xiao, W. 2018. Ridge subduction and slab windows in the Central Asian Orogenic Belt: Tectonic implications for the evolution of an accretionary orogen. *Gondwana Research*, v. 61, p. 73-87.  
<https://doi.org/10.1016/j.gr.2018.05.003>